

# **A UNIFIED MODEL OF SOLID DEPOSITION FROM PETROLEUM FLUIDS INCLUDING WAXES, ASPHALTENES, HYDRATES AND SCALES.**

B. Edmonds, R. A. S. Moorwood\* and R. Szczepanski

Infochem Computer Services Ltd., South Bank Technopark, 90 London Road,  
London, SE1 6LN, U.K.

\* To whom correspondence should be addressed.

Keywords: solid-fluid equilibria, model, petroleum fluid, phase boundary, wax, asphaltene, gas hydrate, scale.

## **Abstract**

A consistent approach to modelling the phase equilibria of solids, liquids and gases is advocated. Examples of complex phase behaviour involving solid depositions from petroleum fluids are presented which have been calculated in this way. Examples include cases where different solid phases are present and affect one another.

## **Introduction**

The oil industry is regularly involved in dealing with complex phase behaviour in the processing of oil and gas streams. The fluid phases which may be encountered include a gas phase, one or two hydrocarbon liquid phases and an aqueous phase. Besides the fluid phases a number of undesirable solids phases can be deposited including pure solids (e.g. ice, solid carbon dioxide etc.), gas hydrates, waxes, asphaltenes and scales. Gas hydrates are clathrates of the components of natural gases in an ice-like crystal lattice. Waxes are a mixture of solid hydrocarbons, normally dominated by paraffinic components and asphaltenes are also an organic deposit but they consist of highly polar heavy aromatics. Scales are somewhat different being mixtures of crystalline inorganic salts. In this paper we present an approach to modelling these effects in a consistent and systematic way that can be used for engineering studies.

## **Computational framework**

### **Phase equilibrium and model library**

In order to solve phase equilibrium problems involving any number or combination of solid, liquid and gaseous phases, the authors have developed an algorithm [1] that systematically searches for the equilibrium phases using a sequence of phase stability tests and phase split calculations as advocated by Michelsen [2]. An important feature of the algorithm is that it allows different models to be used for each type of phase and property that is to be calculated, so that phases with completely different thermodynamic properties can be handled simultaneously. The user initiates phase equilibrium calculations by defining a list of possible phases that should be considered, and specifying the models to be used for each property of each phase. The algorithm operates by making successive calls to a models library for the properties of the phases.

The thermodynamic models in the models library have all to be implemented in a completely uniform way for every possible phase. Our convention is to supply the pressure, temperature and component mole numbers of a phase as inputs and to return the fugacity coefficients and total volumes, enthalpies and entropies. We also return analytical derivatives of all the output quantities with respect to all input quantities for each phase, if required, to support second order solution methods. Care has to be taken to use strictly consistent reference points: for most components, for example, we use the ideal gas state at unit pressure to calculate fugacity coefficients. However, for ionic species a reference state in aqueous solution is more appropriate.

To operate a model library along these lines, it is important in practice to allow model 'chains', where one model can call another. A familiar example is the use of gas phase correction models with activity equations when calculating fugacities. Another example is modelling solid phases where it is often convenient to calculate the thermodynamics of a liquid phase of the same composition, temperature and pressure with one model, and then to add terms for the thermodynamics of solidification with another model.

### **Tracing phase boundaries**

The authors have developed a new multiple phase boundary tracer to help picture complex phase behaviour. Currently available phase envelope routines are usually restricted

to handling vapour-liquid equilibria. In contrast, the new phase boundary tracer can follow the boundary of any phase the user may specify. Because the number of coexisting phases is not fixed, the tracer has to test for the possible appearance and disappearance of phases at every point it calculates. Whenever the coexisting phases change, the phase boundary will show a gradient discontinuity; the tracer locates the point of the discontinuity and searches for the new direction of the phase boundary beyond the discontinuity.

## **Models used**

For the examples in this paper we used either the SRK [3] or Peng-Robinson [4] equations with minor adaptations for the fluid phases. For the hydrate phases we used our own implementation of the Van der Waals-Platteeuw theory [5]. The wax phase model is based on that proposed by Firoozabadi and co-workers [6]. Asphaltenes have been treated as single solid components with thermodynamic properties regressed to match the available data [7]. For scales, we have implemented expressions for the activity coefficients in aqueous solution as a function of temperature and composition [8,9].

The structure of the model library also makes it relatively simple to implement alternative models for any of the solid or fluid phases. However, the main purpose of this paper is to show the advantages of a consistent framework for performing complex phase equilibrium calculations, not to advocate particular thermodynamic models.

## **Examples**

### **Gas hydrates**

Fig. 1 shows a phase diagram for a lean natural gas that contains about 96.8 mol% methane; the phase boundary tracer shows the hydrocarbon vapour-liquid envelope. The water dew point line is also shown starting from the triple point. Below 273.15K, the water line becomes ice, but at higher pressures the ice becomes a structure II gas hydrate [10] owing to the stabilising effect of adsorbed gas. Natural gases normally form structure II hydrates; however, the phase boundary tracer reveals a surprising phase change at about 15MPa. The structure II hydrate line shows a sharp discontinuity and a region of structure I hydrate is found. We believe this is a consequence of the gas's high methane concentration [5].

Fig. 2 shows the model predictions for the hydrates formed by Bush Hill vent gas. Bush Hill vent is located on the sea floor of the Gulf of Mexico and the hydrates formed round the vent are the first example found of naturally occurring structure H hydrate [11]. The hydrate is stabilised by isopentane which is a strong structure H former. The phase diagram shows that the likely conditions subsea just fall in the calculated structure H stability region. We have found several other examples where petroleum fluids will form structure H hydrates with excess water; in every case, structure II hydrate is formed first, but once the structure II formers have been adsorbed, structure H hydrate then starts to form.

### **Hydrates and scales**

The inorganic salts that occur in produced waters associated with oil and gas production are natural hydrate inhibitors. Fig. 3 shows the structure II hydrate line for a natural gas in the presence of pure water and also with the addition of salts. The calculation shows the effect of a mixture of 1.67M sodium chloride and  $6.7 \times 10^{-5}$ M barium sulphate. Although a real produced water will contain other salts, this example illustrates the connection between scaling and hydrate formation. The effect of the salts is to lower the activity of water thereby depressing the ice and hydrate points.

In the absence of hydrate formation, the lowering of the temperature will lead to a point where the barium sulphate will crystallise. i.e. form a scale. Barium sulphate is a prime example of a sulphate scale former. If the formation of hydrates is included in the calculation, as it should be, the scaling prediction has to be revised as the hydrates use up water causing the salts in the aqueous phase to become increasingly concentrated. As the concentration of barium sulphate rises the tendency to form scale increases. A complication is that barium sulphate solubility increases with increasing sodium chloride concentration [9].

### **Waxes**

Fig. 4 shows a simple example of wax-like formation. The experimental data is for a gas condensate to which phenanthrene has been added as a simulated waxing component [12]. Phenanthrene was treated as a single component that is able to solidify. Note that

the wax line shows a marked discontinuity where it crosses the bubble point line owing to the different solubilities of phenanthrene in the liquid and gas phases.

Real waxes are far more difficult to model as they are exceedingly complex mixtures of hydrocarbons. Fig. 5 shows an example of a crude oil reported by W.B.Pedersen et al. [13] as 'Oil 1'. The oil was represented as a series of hydrocarbon pseudocomponents following Firoozabadi's procedure [6]. Each pseudocomponent is considered capable of solidifying independently of the others. The thermodynamic parameters for solidification were also estimated using Firoozabadi's model. Fig. 5 shows the prediction of the model compared with experiment for the amount of wax deposited v. temperature. The model correctly predicts that the rate of wax deposition tends to increase with falling temperature. It also shows that the mass of wax deposited does not increase smoothly but occurs in 'jumps'. This is a feature of the Firoozabadi model: as the temperature falls more of the components start to solidify; as a new component begins to solidify there is an upward jump in the calculated mass of wax deposited.

### **Waxes and hydrates**

A simulated live oil was used to illustrate the ability of the algorithm simultaneously to model the onset of waxes and hydrates. The live oil consists of 'Oil 1' above plus additional gas. Fig. 6 shows the calculated bubble point line, wax appearance line and the hydrate appearance line. In this example more water is present than in Fig. 1. As a result, the bubble point line is noticeably deviated on crossing the hydrate line, as the hydrate adsorbs light gases from the oil lowering the bubble point. At higher pressures the hydrate and wax lines cross.

### **Asphaltenes**

Asphaltenes are another organic material that can be deposited by crude oils. Treating the deposition of asphaltenes as a thermodynamic equilibrium process, we can find the amount of asphaltene deposited by performing a normal phase equilibrium calculation. Fig. 7 shows two isotherms for a crude oil. (The experimental data shows some scatter.) The model reflects the fact that the solubility of asphaltenes is reduced by the presence of light gases; below the bubble point, as gases vaporise, the asphaltene solubility in the

oil rises rapidly. Also, the solubility of asphaltene in this example falls with rising temperature, although the opposite occurs in some oils.

Fig. 8 shows the calculated asphaltene deposition envelope (ADE) for the same oil as a function of methane content. An interesting feature of the model is that it predicts that asphaltene will redissolve at higher temperatures, although the asphaltenes would in practice decompose before reaching these temperatures.

## Conclusions

The examples in this paper have been chosen to demonstrate that it is possible to model all the phase behaviour encountered when processing petroleum fluids in a unified and consistent way. It is possible to see what the influence of one type of solid deposition will be on another, e.g. waxes on hydrates. It is also possible to provide alternative models for particular phases for comparison purposes. Finally, by treating all models and phases on an equal footing, it simplifies the task of writing interfaces to access the model from applications programs.

## References

1. J. F. Counsell, R. A. S. Moorwood, R. Szczepanski: 'Calculating Multiphase Equilibria', presented at VLE '90 Conference, Aston University, U.K., June 1990.
2. M. L. Michelsen: *Fluid Phase Equil.*, **9**, 1 and 21, (1982).
3. G. Soave: *Chem. Eng. Sci.*, **27**, 1197, (1972).
4. D.-Y. Peng, D. B. Robinson, *Ind. Eng. Chem. Fundam.*, **15**, 1, (1976); *ACS Symp. Ser.*, **133**, 193, (1980).
5. E. M. Hendriks, B. Edmonds, R. A. S. Moorwood, R. Szczepanski: *Fluid. Phase. Equil.*, **117**, 193, (1996).
6. C. Lira-Galeana, A. Firoozabadi, J. M. Prausnitz: *A. I. Ch. E. J.*, **42**, 239, (1996).
7. B. Edmonds, R. A. S. Moorwood, R. Szczepanski: 'Predicting Solid-Fluid Equilibria: Industrial Applications', presented at VLE '90 Conference, Aston University, U.K., June 1995.
8. J. W. Tester, M. Modell: 'Thermodynamics and Its Applications', 3rd. ed., Prentice Hall, New Jersey, (1997).
9. C. C. Templeton: *J. Chem. Eng. Data*, **5**, 514, (1960).
10. E. D. Sloan, Jr.: 'Clathrate Hydrates of Natural Gases', Dekker, New York, (1990).
11. R. Sassen, I. R. MacDonald: *Org. Geochem.*, **22**, 1029, (1994).

12.P. Ungerer, B. Faissat, C. Leibovici, H. Zhou, E. Behar, G. Moracchini, J. P. Courcy: *Fluid Phase Equil.*, **111**, 287, (1995).

13.W. B. Pedersen, A. B. Hansen, E. Larsen, A. B. Nielsen, H. P. Rønningsen: *Energy and Fuels*, **5**, 908, (1991).

Figure 1: phase diagram for a natural gas showing water and hydrate regions

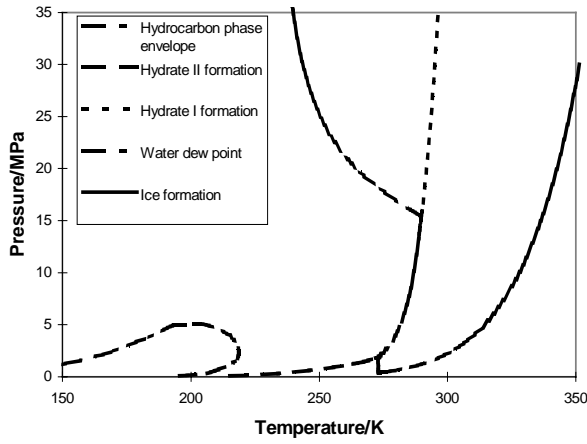


Figure 2: Bush Hill vent gas phase diagram

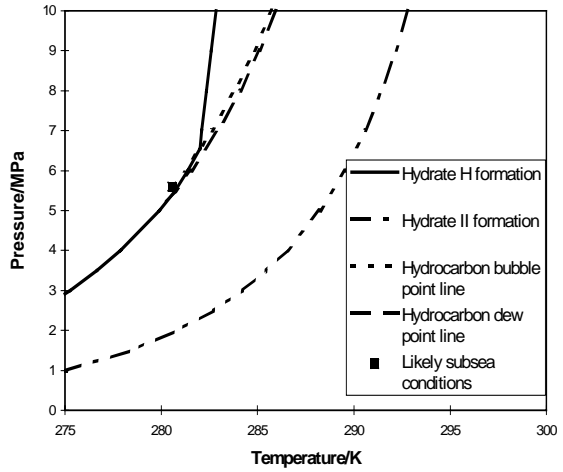


Figure 3: phase diagram for a natural gas and water with NaCl and BaSO4

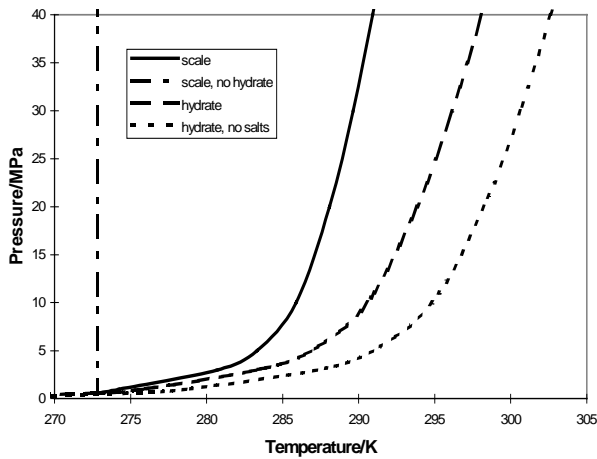


Figure 4: phenanthrene deposition

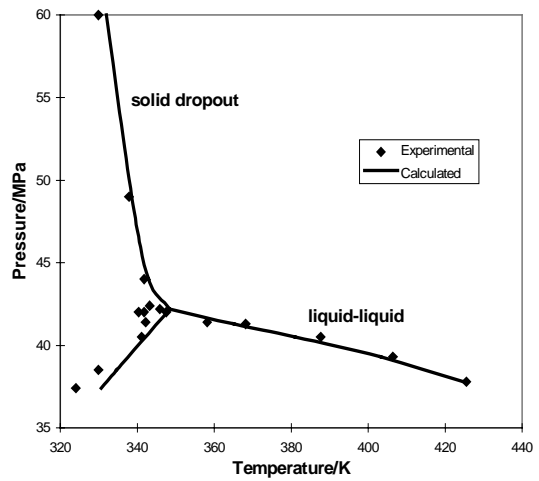


Figure 5: wax deposition for 'Oil 1'

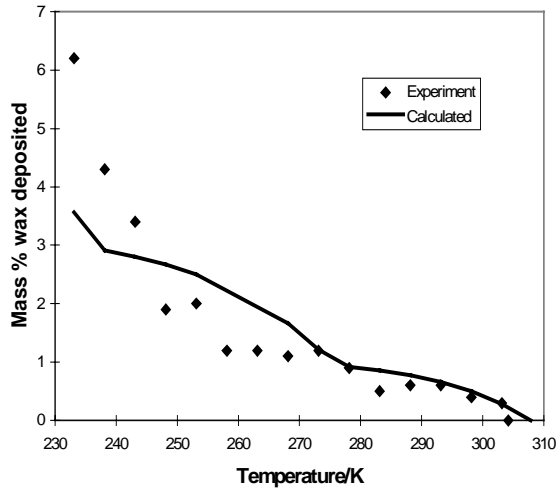


Figure 6: phase diagram for 'Oil1' with added gas and water

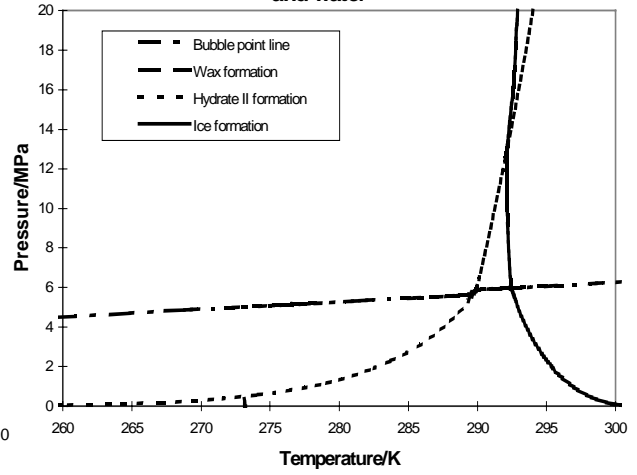


Figure 7: asphaltene deposition

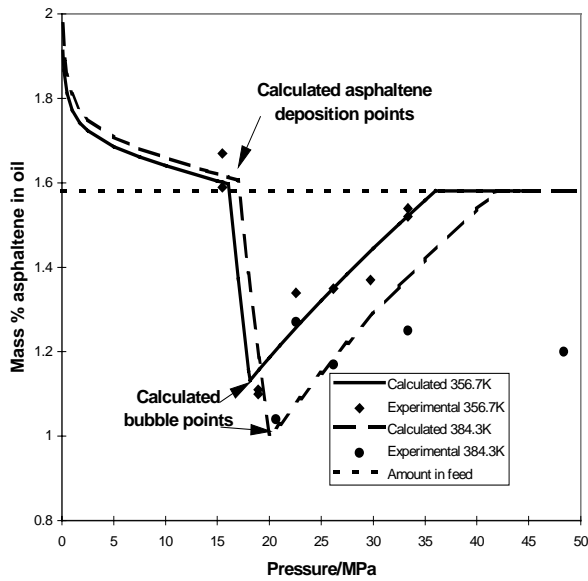


Figure 8: ADEs and bubble point lines for oil with varying methane content

